J. Physiol. (1979), **291**, *pp.* 75–100
With 1 *plate and* 11 *text-figures*
Printed in Great Britain

ELECTRICAL COUPLING BETWEEN CONES IN TURTLE RETINA

BY P. B. DETWILER* AND A. L. HODGKIN

*From the Physiological Laboratory, University of Cambridge, and the *Department of Physiology and Biophysics, School of Medicine, University of Washington, Seattle, U.S.A.*

(*Received 30 August 1978*)

SUMMARY

1. The electrical coupling between cones of known spectral sensitivity in the peripheral part of the turtle's retina was studied by passing current through a micro-electrode inserted into one cone and recording with a second micro-electrode inserted into a neighbouring cone.

2. Spatial sensitivity profiles were determined by recording flash responses to a long narrow strip of light which was moved across the impaled cones in orthogonal directions. These measurements gave both the length constant λ of electrical spread in the cone network and the separation of the two cones.

3. The cone separation determined from the spatial profiles agreed closely with that measured directly by injecting a fluorescent dye into two cones.

4. The length constant λ varied from 18 to 39 μm with a mean of 25 μm for red-sensitive cones and 26 μm for green-sensitive cones.

5. The majority of cone pairs studied were electrically coupled provided they had the same spectral sensitivity and were separated by less than 60 μm: thirty-two out of thirty-six red–red pairs, two out of two green–green pairs, none out of eight red–green pairs: no blue cones were observed.

6. The strength of electrical coupling was expressed as a mutual resistance defined as the voltage in one cell divided by the current flowing into the other. Mutual resistances decreased from a maximum value of about 30 MΩ at separations close to zero to 0·2 MΩ, the lower limit of detectable coupling at separations of about 60 μm. Mutual resistances were always positive and were independent of which cell was directly polarized. The coupling seemed to be ohmic and any rectification or non-linearity probably arose in the cone membranes rather than in the coupling resistances.

7. The results were analysed in terms of the Lamb & Simon (1977) theories of square and hexagonal lattices, which approximate to the continuous sheet model except in the case of the cone to which current is applied.

8. The total membrane resistance of a single cone was estimated as 100–300 MΩ and the connecting resistances as 100 MΩ for a square array and 170 MΩ for a hexagonal array. The input resistance of a cone in the network was 25–50 MΩ. Lower values were often obtained but may be due to injury by the micro-electrodes.

9. The time constant of an isolated cone was estimated as about 20 msec and the capacity as about 100 pF.

10. Discrepancies between experimental findings and theoretical predictions of

0022-3751/79/3460-0709 $01.50

the hexagonal or square array models were tentatively attributed to an overestimate of λ resulting from light scattering.

INTRODUCTION

Several years ago Baylor, Fuortes & O'Bryan (1971) demonstrated electrical coupling between cones in the peripheral turtle retina. They found that current applied through a microelectrode in one cone often caused an electrical change in an adjacent cone provided the two cones were separated by a distance less than about 40 μm. A similar result was obtained in the rods of the snapping turtle by Copenhagen & Owen (1976) who reported electrical coupling over distances of up to about 120 μm. In both rods and cones the effect was usually of the kind expected from a simple electrical connexion between the two receptors. Thus, the polarity of the voltage change evoked by current applied to one cone is normally the same in both cones; it occurs with both hyperpolarizing and depolarizing current and is symmetrical in that a voltage of the same size is recorded if the voltage and current electrodes are interchanged. The relation between applied current and voltage is not linear, but the deviations that occur can be attributed to non-linearities in the membrane of the photoreceptor rather than to any non-linearity in the connecting elements. The only exception to this simple type of behaviour is that Baylor *et al.* (1971) once observed reverse coupling, i.e. current caused a potential change in one cone of a sign opposite to that expected from the direction of the current applied to the other.

Experiments with two electrodes placed in neighbouring cones are difficult to carry out and this probably accounts for the fact that a number of simple but important questions regarding cone coupling have remained unanswered. Thus Baylor & Hodgkin (1973) obtained indirect evidence that cones were coupled if they had the same spectral sensitivity but not otherwise. Their conclusion, which was based on the spectral sensitivities of red- and green-sensitive cones, clearly needs checking by direct measurements with two electrodes. It was also of interest to find out whether all cones of the same spectral sensitivity within a certain radius are coupled together or whether coupling is a somewhat random affair. Finally, it seemed important to obtain quantitative evidence on the relation between coupling and distance since this should enable calculations to be made of the membrane resistances of individual cells and of the resistances coupling them together.

METHODS

Preparation

Experiments were performed on the retina of red-eared swamp turtles, *Pseudemys scripta elegans*. The eye was removed, hemisected, and drained of vitreous as described by Baylor *et al.* (1971). The posterior half of the eye was placed in a moist recording chamber and optimally positioned for penetrating cells in the peripheral portion of the dorsal retina. The eye cup was maintained at room temperature in a stream of moist 95 % O_2, 5 % CO_2.

Cell penetration

Simultaneous intracellular recordings from two cones were obtained with separate electrodes mounted on independent micromanipulators. The electrodes were positioned initially within 10–30 μm of each other on the vitreal surface, and were then advanced into the retina in parallel, taking alternate steps of roughly equal size. We determined the distance between cone pairs by moving a narrow strip of light (5 μm by 1·55 mm) across the retina and plotting the response amplitude of each cell as a function of strip position. Complete strip scans were done along orthogonal axes, the cell centres were expressed in terms of rectangular co-ordinates, and the cell separation was calculated.

To assess the accuracy of this method, we sometimes marked the location of each member of a cell pair with an intracellular dye and directly measured the distance between stained cells using a compound microscope. The electrodes were filled with a 4 % solution (w/v, distilled water) of Lucifer yellow, a new, highly fluorescent dye developed by Stewart (1978). Dye was iontophoresed by negative current pulses (5–10 nA; 500 msec) applied at 0·5 Hz for 5–10 min. The tissue was fixed in 4 % formaldehyde, pH 7·4, and viewed in a Vickers epifluorescence microscope. By using incident illumination we could observe dye-marked cells without 'peeling' the retina from the pigment epithelium; this was an advantage because the process of isolating the retina might alter the relative position of the injected cells. Cell shrinkage due to fixation was neglected (Baylor & Fettiplace, 1975).

After measuring the separation between marked cells, the tissue was dehydrated, embedded in paraffin and sectioned to verify that the dye-injected cells were cones.

Electrical recording

Electrodes were pulled on a Livingston-type horizontal puller from Omega Dot capillary tubing (Glass Company of America), which has a round ridge fused to the inside wall to promote filling. Electrodes contained 4 M-potassium acetate adjusted to pH 7·4 and had resistances between 200 and 400 MΩ. Electrodes filled with 4 % Lucifer had resistances between 1000 and 1500 MΩ. The electrodes were connected to high-impedance, negative-capacitance pre-amplifiers which permitted voltage control of the current passed through the recording electrode (Colburn & Schwartz, 1972). Injected current was calculated from the voltage drop across a 50 MΩ feed-back resistor in a virtual ground circuit. Capacitative interactions between electrodes were reduced by shielding one of the electrodes with a grounded stainless-steel sleeve. Data were recorded on an FM tape recorder with a band width of d.c. to 1250 Hz.

We tested pairs of impaled cones for direct electrical coupling by passing current into one cone and recording voltage from the other. The degree of coupling is expressed as a mutual resistance (R_μ), defined as the intracellular voltage change in one cell divided by the current applied to the other cell. The component of mutual resistance due to extracellular current flow was measured by withdrawing one electrode to a just extracellular position and injecting the same current through the remaining intracellular electrode. This procedure was followed for each cone pair. The measured extracellular resistances were somewhat variable but averaged about 0·1 MΩ. Thus pairs with mutual resistances of 0·1 MΩ or less were classified as uncoupled.

Light stimuli

An optical bench of the Baylor & Hodgkin (1973) design was used to form a reduced (1/21) image of a variable field aperture on the retina. The aperture was mounted on micrometer-driven cross carriages and its position monitored by vertical and horizontal dial indicators. The image quality of the optical stimulator was evaluated by the method of Baylor & Hodgkin (1973) and, after elimination of one defect, was found to be as sharp as in their experiments and in those of Lamb & Simon (1976, Fig. 1). In our initial experiments the image was slightly distorted by a low-quality prism, and this defect apparently led to values of space constant about 50 % greater than normal; these have not been included in the averages (see notes to Table 3). Light intensity was measured periodically between the experiments with a calibrated silicon photodiode (United Detector Technology Inc. 40X Optometer) placed at the position of the retina. The unattenuated irradiance of light passed through a narrow-band, 650 nm interference filter was $1{\cdot}55 \times 10^3$ erg cm^{-2} sec^{-1} (mean of five measurements).

THEORY AND METHOD OF ANALYSIS

This section shows how the analysis of Lamb & Simon (1976), together with some convenient approximations, can be used to calculate basic constants from measurements of the separation and mutual resistance of pairs of cones.

It is assumed that cones are arranged in a regular hexagonal or square array. The hexagonal array is probably more realistic (p. 90), but it is useful to consider the square array as well, partly because it is simpler to think about and partly because consideration of two networks shows whether theoretical predictions are likely to depend critically on the geometrical assumptions that have to be made.

The resistance between the inside and outside of an electrically isolated cone is denoted by r_m (Ω), and the resistance of a single junction between cones by r_s (Ω). For many purposes a convenient approximation is to replace the discontinuous lattice with a continuous model consisting of a two-dimensional lamina with a sheet resistance, R_s (Ω), and a leakage resistance, R_m (Ω cm^2). If there are N cones per unit area and $D(= 1/\sqrt{N})$ is the effective cell spacing, then the leakage resistance, R_m of the sheet is given by

$$R_m = r_m D^2. \tag{1}$$

In the square array D is equal to the distance, d, between adjacent cones, but in the hexagonal array

$$D^2 = \frac{\sqrt{3}}{2} d^2. \tag{2}$$

In the square array the sheet resistivity, R_s, is equal to r_s, but in the hexagonal array

$$R_s = r_s/\sqrt{3}. \tag{3}$$

When the retina is illuminated by a strip the potential on either side of the illuminated band should fall off exponentially with a space constant, λ, which is given by

$$\lambda^2 = R_m/R_s. \tag{4}$$

For the continuous model eqn. (4) is exact, but for the discontinuous model it is an approximation, and should strictly be replaced by the following equations for the square and hexagonal array, respectively (see Lamb & Simon, 1976).

$$\gamma = \frac{r_s}{r_m} = 2 \cosh \left(\frac{D}{\lambda}\right) - 2 \tag{5}$$

$$\gamma = \frac{r_s}{r_m} = 4 \cosh \left[\left(\frac{\sqrt{3}}{2}\right)^{\frac{1}{2}} \frac{D}{\lambda}\right] - 4. \tag{6}$$

However if $\lambda > D$, as in nearly all our experiments, use of eqn. (4) does not lead to errors greater than 5 or 10%.

We must now consider the distribution of potential when current is injected into a single cell. Text-fig. 1*A* and *B*, which were computed from eqns. (12) and (18) of Lamb & Simon (1976) by a programme written by Dr Lamb, show the distribution of potential in the square and hexagonal arrays. Lamb & Simon's equations for the

potential at the node m, n are

$$\frac{V_{m,n}}{i_0 r_m} = \gamma \int_0^\infty I_m(2T)\, I_n(2T)\, e^{-(\gamma+4)T}\, dT, \tag{7}$$

for the square array, and

$$\frac{V_{m,n}}{i_0 r_m} = \gamma \int_0^\infty \left\{ \sum_{k=-\infty}^{\infty} I_{m+k}(2T)\, I_k(2T)\, I_{n-k}(2T) \right\} e^{-(\gamma+6)T}\, dT, \tag{8}$$

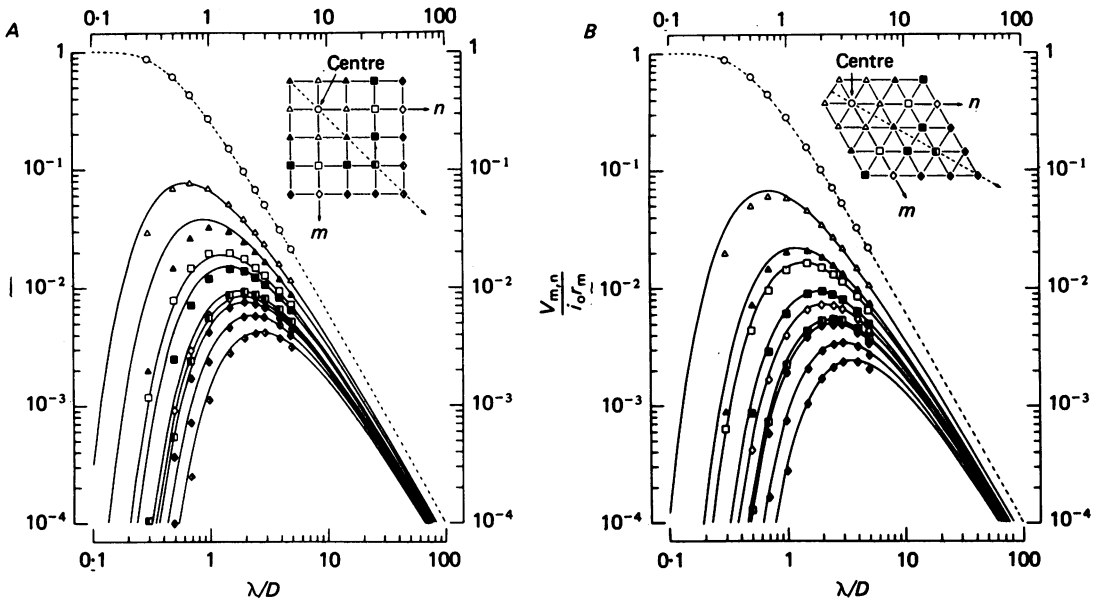

Text-fig. 1. *A*, spread of potential in a square lattice. The points were computed from eqn. (7) (see Lamb & Simon, 1976, eqn. (12)); the ordinate gives the potential at the m, n cell as a fraction of the potential that would be recorded with the same current applied to an isolated cell i.e. $V_{m,n}/i_0 r_m$; the abscissa is λ/D, where λ is the space constant and $D = 1/\sqrt{N}$ is the effective cell spacing, N being the number of cones per unit area. The continuous curves which are an approximate fit to the points, were computed by eqn. (10). The broken curve for $V_{0,0}$ was calculated by eqn. (11). Current was applied to the centre cell and voltage recorded at the different lattice positions indicated by the key to the symbols on the inset. The lattice is symmetric about the dashed line. Note that $d = D$ and that γ can be obtained from D/λ by eqn. (5); r/λ can be obtained as $(n^2+m^2)^{\frac{1}{2}} d/\lambda$.

B, similar to *A* but showing the spread of potential in a hexagonal lattice; the points were computed from eqn. (8) and the continuous curves from eqn. (10) (as above). The broken curve for $V_{0,0}$ was computed by eqn. (12).

Note that d can be obtained from D by eqn. (2), γ from D/λ by eqn. (6); r/λ as $(n^2+m^2+nm)^{\frac{1}{2}} d/\lambda$.

for the hexagonal array. In the square array m and n are measured along orthogonal axes, and in the hexagonal array, along axes at an angle of 60°; $\gamma = r_s/r_m$, $I_\nu(\ )$ is a modified Bessel function of the νth order; $V_{0,0}$ is the voltage at the origin where the current i_0 is applied. In Fig. 1 the symbols are exact values computed from these two equations, and the continuous lines were calculated from the relatively simple

equations of the continuous-sheet model. As shown by Jack, Noble & Tsien (1975) and Lamb (1976), when a current i_0, is injected at $r = 0$ the potential at r is

$$\frac{V_r}{i_0} = R_s \frac{K_0(r/\lambda)}{2\pi}, \tag{9}$$

where K_0 is a modified Bessel function. From eqns. (1) and (4) this can also be written as

$$\frac{V_r}{i_0 r_m} = \frac{D^2}{\lambda^2} \frac{K_0(r/\lambda)}{2\pi}. \tag{10}$$

The continuous lines in Text-fig. 1, which were calculated by this formula, can be seen to be a reasonable approximation to the hexagonal array for $\lambda/D > 0{\cdot}5$, and the square array for $\lambda/D > 1$.

Eqn. (9) predicts an infinite potential at $r = 0$ and cannot be applied to the cell where current is applied. For the square grid the exact expression given by Lamb & Simon (1976) in their eqn. (15) is shown by the interrupted line in Text-fig. 1*A*; the equation, given for reference, is

$$\frac{V_{0,0}}{i_0 r_m} = \frac{2}{\pi}\left(\frac{\gamma}{\gamma+4}\right) K\left(\left[\frac{4}{\gamma+4}\right]^2\right), \tag{11}$$

where $K(x)$ is the complete elliptic integral of the first kind. For the hexagonal grid the interrupted line in Fig. 1*B*, which gives the potential in the cell where current is applied, was calculated by the following equation, which turns out to be a very good approximation:

$$\frac{V_{0,0}}{i_0 r_m} = \frac{\gamma + 6V_{1,0}/(i_0 r_m)}{\gamma+6} \tag{12}$$

where $\gamma = r_s/r_m$, $V_{0,0}$ is the potential at the origin, and $V_{1,0}$ is the potential in the first ring of cells calculated by eqn. (9). Eqn. (12) can be derived simply by application of Kirchoff and Ohm's Law to the hexagonal network.

Application of these expressions to the results is best illustrated by a specific example. It was found that a pair of red-sensitive cones, which were separated by 28·3 μm, had a mean λ of 27·6 μm and a mutual resistance (i.e. V_r/i_0) of 3·05 MΩ. If D, the effective mean distance between red-sensitive cones, is taken as 17·4 μm from the measurements of Baylor & Fettiplace (1975) (see Lamb & Simon, 1976), then from eqn. (10) r_m is found to be 119 MΩ. Similarly, from eqns. (1) to (4) the coupling resistance, r_s, is found to be 82 MΩ for the hexagonal array and 47 MΩ for the square array. From the values of λ/D and r_m and from Text-fig. 1, the input resistance, $V_{0,0}/i_0$, is found to be 16·8 MΩ for the hexagonal array and 16·4 MΩ for the square array.

Text-fig. 2 illustrates the validity of the $K_0(\ )$ approximation in a different way. Here values of $\frac{\lambda^2 V_{m,n}}{D^2 i_0 r_m}$, calculated as in Text-fig. 1, are plotted on a logarithmic scale against r/λ. Both hexagonal and square arrays were considered and the ratio λ/D was given values of 3, 2, 1 and 0·7. The curve is for the continuous-sheet model, where eqn. (10) applies; the ordinate is then $K_0(r/\lambda)/2\pi$. Provided $\lambda/D > 1$, this curve is close to all the points except at the origin.

Two points of practical importance arise from this graph. First if $\lambda/D > 1$ and the current and voltage electrodes are in different cells, then it is clear that little error should arise in using eqn. (10) to calculate λ and hence r_m. Secondly, we can test the idea that all cones have the same value of r_m, but that coupling resistance varies, by seeing whether a plot of $\frac{\lambda^2 V_{m,n}}{D^2 i_0}$ is fitted by the continuous curve in Fig. 2. The results of this test are given in Text-fig. 7 and discussed on page 92.

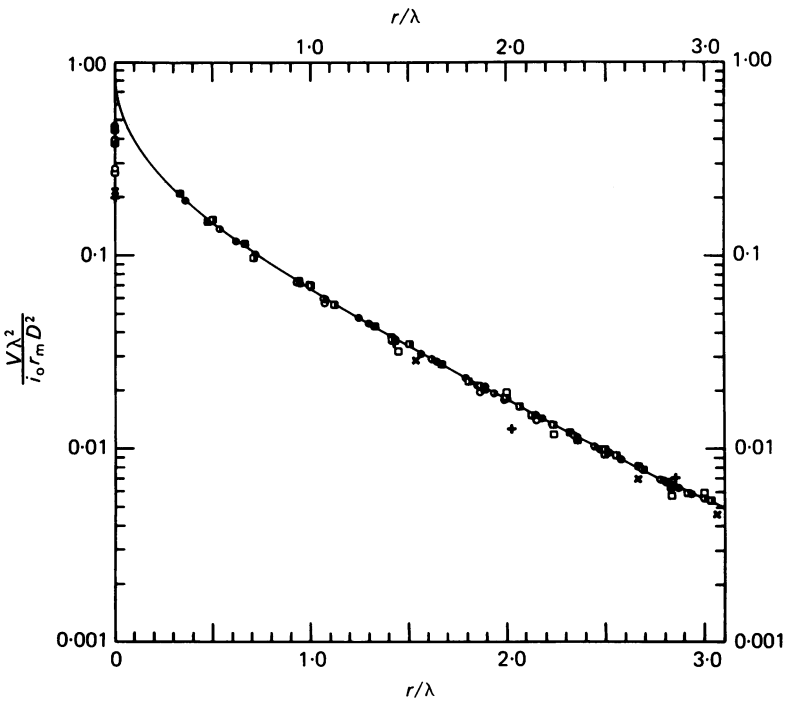

Text-fig. 2. Theoretical distribution of potential for different values of λ/D in the hexagonal and square arrays and in the continuous sheet model. The abscissa is r/λ and the ordinate is $\frac{V_{m,n}\lambda^2}{i_0 r_m D^2}$ for the values of λ/D shown below.

λ/D	Square	Hexagonal
3	■	●
2	◨	◑
1	□	○
0·7	+	×

The curve is $\frac{1}{2\pi} K_0(r/\lambda)$ and gives $\frac{V}{i_0 r_m}\frac{\lambda^2}{D^2}$ for the continuous sheet model (see eqn. (10)). Only the points on the axis and the diagonals are given for the ■ case.

Determination of time constant of cells in a network

In the theory of Lamb & Simon (1976) the variable T in eqns. (7) and (8) is equal to $t/\gamma\tau$ where t is time, $\gamma = r_s/r_m$ and τ ($= r_m c_m$) is the time constant of an individual cell in the network. If the upper limit of the integral in eqns. (7) and (8) is taken as γT instead of ∞, we can obtain the time course of the rise of potential at any given node when a constant current is applied to the node at the origin. This provides a theoretical basis for estimating τ from the experimental data.

TABLE 1. Theoretical values of $V_{m,n}/i_o r_m$ at different times in a hexagonal network

t/τ	Node →	(0, 0)	(1, 0)	(1, 1)	(2, 0)	(2, 1)	(3, 0)	(2, 2)	
↓	r/d →	0·0	1·0	1·73	2·0	2·65	3·00	3·46	
0·1		0·0818	0·0021	0·0001	0·0001	0·0000	0·0000	0·0000	$\lambda/D = 1$
0·2		0·1363	0·0068	0·0005	0·0003	0·0000	0·0000	0·0000	
0·5		0·2176	0·0230	0·0034	0·0020	0·0003	0·0002	0·0000	
1·0		0·2585	0·0409	0·0098	0·0063	0·0017	0·0009	0·0003	
∞		0·2802	0·0570	0·0197	0·0144	0·0062	0·0040	0·0023	
0·1		0·0681	0·0040	0·0003	0·0002	0·0000	0·0000	0·0000	$\lambda/D = 1·5$
0·2		0·1001	0·0107	0·0016	0·0009	0·0001	0·0001	0·0000	
0·5		0·1336	0·0260	0·0074	0·0049	0·0015	0·0008	0·0003	
1·0		0·1478	0·0369	0·0142	0·0105	0·0045	0·0029	0·0015	
∞		0·1563	0·0448	0·0205	0·0162	0·0089	0·0065	0·0044	
0·1		0·0546	0·0054	0·0007	0·0004	0·0001	0·0000	0·0000	$\lambda/D = 2·0$
0·2		0·0722	0·0122	0·0028	0·0018	0·0005	0·0002	0·0001	
0·5		0·0883	0·0232	0·0091	0·0067	0·0029	0·0018	0·0009	
1·0		0·0956	0·0297	0·0142	0·0112	0·0061	0·0044	0·0028	
∞		0·1002	0·0341	0·0181	0·0149	0·0092	0·0073	0·0053	
				Continuous sheet approximation					
0·1			0·0067	0·0007	0·0003	0·0000	0·0000	0·0000	$\lambda/D = 2·0$
0·2			0·0138	0·0033	0·0019	0·0004	0·0002	0·0000	
0·5			0·0242	0·0098	0·0071	0·0031	0·0019	0·0010	
1·0			0·0303	0·0147	0·0115	0·0063	0·0045	0·0029	
∞			0·0344	0·0185	0·0151	0·0094	0·0074	0·0054	

The first three blocks of numbers were calculated from eqn. (8) and the fourth block from eqn. (14). τ ($= r_m c_m$) is the time constant of an individual cell in the network. Note that D^{-2} is the number of 'nodes' per unit area and that D is related to d (the internodal distance) by eqn. (2); $r/d = (n^2+m^2+nm)^{\frac{1}{2}}$.

Table 1 gives values of $V_{m,n}$ at $t/\tau = 0·1$, 0·2, 0·5, 1 and ∞ for nodes near the origin with different values of λ/D. When $\lambda/D > 2$ and $r \neq 0$ the time course approximates closely to that calculated for a continuous sheet which obeys the equation

$$\lambda^2\left\{\frac{1}{r}\frac{\partial}{\partial r}\left(r\frac{\partial V}{\partial r}\right)\right\} = V+\tau\frac{\partial V}{\partial t}. \tag{13}$$

It can be shown by standard methods (Carslaw & Jaeger, 1959; Jack *et al.* 1975) that the solutions of eqn. (13) for a current i_0 applied at $r = 0$ at $t = 0$ is

$$V = \frac{i_0 R_m}{4\pi\lambda^2}\int_0^{t/\tau}\frac{\tau}{t'}\exp\left[-\frac{r^2\tau}{4\lambda^2 t'}-\frac{t'}{\tau}\right]\mathrm{d}\left(\frac{t'}{\tau}\right). \tag{14}$$

When this equation is applied as an approximation to the discontinuous case R_m is replaced by $r_m D^2$. Comparison of the last two blocks in Table 1 shows that for $\lambda/D = 2$ and $r \neq 0$ eqn. (14) is a good approximation to eqn. (8).

For $\lambda/D < 1{\cdot}5$ and $t/\tau < 0{\cdot}1$ the rise of potential at the origin in the hexagonal network can be calculated with reasonable accuracy by solving the second order equation that results from the assumption that cells further out than the first ring of six are grounded. On this basis if a constant current i_o is applied at $m = n = 0$, then

$$\frac{V_{o,o}}{i_o r_m} = k + \frac{1+bk}{a-b} e^{at/\tau} + \frac{1+ak}{b-a} e^{bt/\tau}, \tag{15}$$

where

$$k = \frac{4\gamma+\gamma^2}{\gamma^2+10\gamma+18} \quad \text{and} \quad \begin{matrix} a \\ b \end{matrix} = -\left\{1+\frac{5}{\gamma} \pm \frac{1}{\gamma}\sqrt{7}\right\}.$$

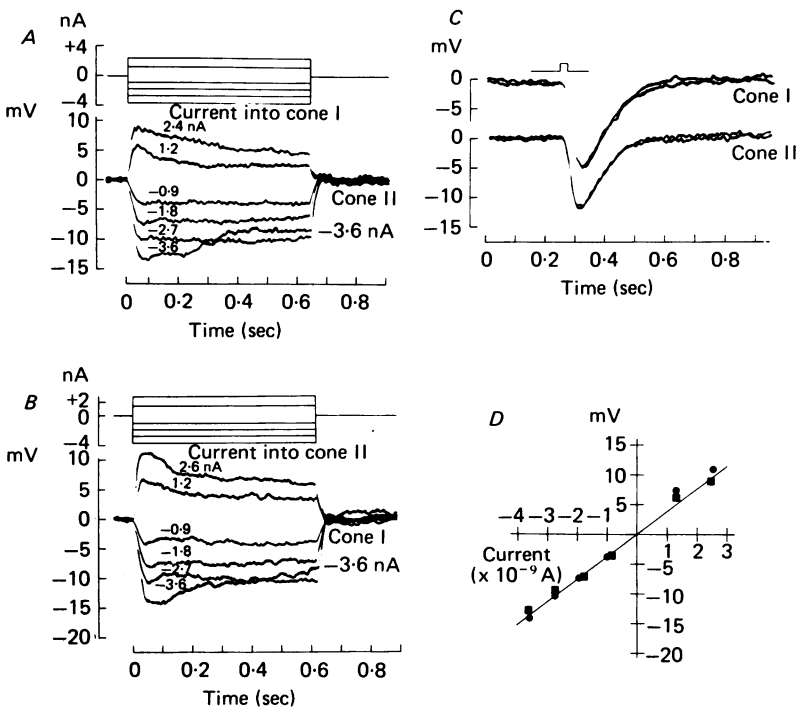

Text-fig. 3. Electrical coupling between simultaneously impaled red-sensitive cones. *A* and *B*, currents applied to one cell produced the illustrated voltage changes in the other cell. In *A* current was passed into cone I and the voltage change recorded from cone II. The location of the current and voltage electrodes was reversed in *B*. During the passage of current the voltage trace of the directly polarized cell went off scale and is not illustrated in either *A* or *B*. *C*, superposed light responses before and after passing currents. The stimulus, an 880 μm radius spot of white light, delivered the equivalent of $9{\cdot}4 \times 10^2$ photons at 644 nm/μm^2 (see Baylor & Hodgkin (1973) for details). *D*, voltage current relation of the coupled pair. The squares and circles plot on the ordinate the peak voltage change in *A* and *B*, respectively, as a function of applied current. The slope of the straight line (fitted by eye) measures the mutual resistance (4·2 MΩ). Cell separation 22 μm. V_{max}: cone I 20 mV, cone II 17 mV. Temperature 23·2 °C.

RESULTS

A typical experiment

Text-figs. 3 and 4 illustrate the basic information, which was collected from as many pairs of cones as possible. In this instance both cones were red-sensitive and, as determined from Text-fig. 4, they were separated by 22 μm. The families of records in Text-fig. 3*A* and *B* show the voltage wave forms given by rectangular pulses of current. It is evident that there is a delayed increase of conductance with

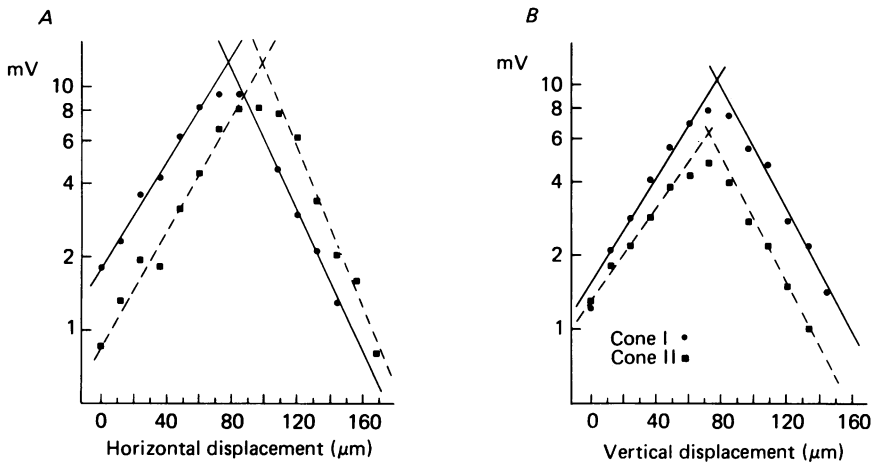

Text-fig. 4. Spatial sensitivity profiles for a pair of red cones. The circles and squares (cone I and II of Fig. 3 respectively) plot response amplitude (mean of four measurements) against the position of a strip of light 1·55 mm long by about 5 μm wide. In *A* the long axis of the strip was vertical and moved horizontally at the level of the optical bench, and in *B* it was horizontal and moved vertically. Length constants were determined from the slope of the straight lines, which were fitted to the points by eye. The intersection of each pair of lines located the cell centre on that axis. From this information the cell separation was calculated to be 22 μm. The stimulus was a 10 msec flash of white light that delivered the equivalent of $3{\cdot}8 \times 10^3$ 644 nm photons μm^{-2} at 2 sec intervals.

both inward and outward currents; this was usually much more conspicuous for the outward, depolarizing currents and was seen when both electrodes were in the same cell. This indicates that the effect is caused by an increase in membrane conductance rather than by a decrease in the conductance of the links between cones. From the graph in *D* where the peak voltage is plotted against current it can be seen that the peak voltage was proportional to current over the range of currents employed. From the coincidence of squares and circles in the Figure, it is apparent that reversing the current and voltage electrodes made no difference in the size of the response, as would be expected if the two cells were connected by a simple ohmic resistance.

The slope of the line relating maximum voltage to current, which is a measure of the mutual resistance, was found to be 4·16 MΩ.

The distance between the cells was determined by movement of a 5 μm wide strip of light across the retina, first in a horizontal and then in a vertical plane. The logarithm

of the response amplitude was plotted against distance, as in Text-fig. 4 and the position of the maximum was taken as the intersection of the two straight lines drawn through the outer portion of the spatial profile. From Text-fig. 4, the separation of the cones was obtained as 22 μm and the mean space constant as 34 μm (determined from the mean slope of the eight straight lines in Text-fig. 4, i.e. 32·4, 32·4, 26·4, 38·4 μm in cone 1 and 46·8, 34·8, 25·2, 36 μm in cone 2).

TABLE 2. Test of method of measuring distance between cones

Separation from slit runs (μm)	Separation from dye injection (μm)	Mutual resistance (MΩ)
97	103	0
80	85	0
108	98	0
54	55	0
25	23	1·9
0	0*	17·8

* Only one cone marked.

Test of the method for measuring cone separation

In a separate series of experiments we assessed the accuracy of the strip procedure for determining cell separation by marking the cells with an intracellular dye. These experiments involved recording from pairs of cells with electrodes containing the fluorescent dye Lucifer yellow. Cell separation was measured by the strip method and then both cones were injected with dye. The entire eyecup was fixed in formaldehyde and examined in an epifluorescence microscope. When viewed through the proximal cellular layers of the retina the stained cells appeared as blurred circular spots (Pl. 1*A*); subsequent histology confirmed these to be cones (Pl. 1*B*). By focusing up and down it was possible to determine the centre of each mark and to measure the distance between centres. The separations measured by the strip procedure and by dye injection were compared in six experiments using red-sensitive cones (Table 2) and were found to be in excellent agreement.

Qualitative consideration of results

Text-fig. 5 and Table 3 summarize the results of all the experiments in which we were able to measure the mutual resistance and distance between pairs of cones separated by less than 90 μm. Pairs were considered to be uncoupled if their mutual resistance was less than 0·1 MΩ, the smallest quantity that could be detected reliably.

The symbols in Text-fig. 5 represent forty-two pairs of red-sensitive cones, two pairs of green-sensitive cones, and ten mixed red–green pairs. The Figure and Table 4 show that none of the red–green pairs were coupled, that both the green pairs were coupled, and that thirty-two out of the forty-two red pairs were coupled; of the eight uncoupled red pairs only four were separated by distances less than 60 μm. Without relying on statistics we can see that the graph provides evidence that coupled cones have the same spectral sensitivity, i.e. red is coupled to red and green to green, but not red to green.

Table 3. Basic constants of coupled pairs

Pair no.	Separation (μm)	$\bar{\lambda}$ (μm)	R_μ (MΩ)	r_m (MΩ)	R_m (Ωcm^2)	R_s (MΩ)	r_s (MΩ)	square r_{in} (MΩ)	hexagonal r_{in} (MΩ)
				Red-sensitive cone pairs					
1	15	25*	18	290	878	141	243	45	48
2	26	30	6·9	247	748	85	147	30	32
3	18	29	9·7	223	675	80	139	27	30
4	0	25	36·0	215	651	106	183	34	36
5	22	31	5·8	173	525	53	92	19	21
6	15	29	9·2	173	524	65	112	22	24
7	4	37	14·2	173	523	39	67	15	16
8	11	25*	13·2	170	515	82	143	26	28
9	12	25*	11·7	158	477	76	132	24	26
10	22	25	5·6	146	422	71	123	23	24
11	22	34	4·2	135	410	36	61	13	14
12	44	33	1·6	135	408	37	64	14	15
13	28	28	3·1	119	359	47	82	16	17
14	55	33	0·86	112	340	31	53	11	12
15	0	25*	17·8	108	327	52	91	17	18
16	21	25*	4·2	101	307	49	85	16	17
17	24	28	2·8	84	255	34	58	11	12
18	25	25*	2·8	83	251	40	69	13	14
19	52	25*	0·65	81	246	39	68	13	14
20	25	21	2·8	77	234	53	91	16	17
21	32	22	1·6	72	218	45	78	14	14
22	29	25	1·5	58	176	28	49	9	10
23	25	24	1·9	57	172	31	53	10	10
24	59	27	0·3	50	151	20	35	7	7
25	29	25	1·3	49	149	24	41	8	8
26	61	30	0·28	47	143	16	27	6	6
27	20	25	1·9	43	127	21	37	7	7
28	22	26	1·4	37	111	17	30	6	6
29	40	25	0·5	33	101	16	28	5	5
30	23	24	1·2	32	98	18	30	5	6
31	19	29	0·5	12	36	4	8	2	2
32	22	18	0·2	4	12	4	6	1	1
Mean	26	27	6	109	330	46	79	15	16
				Green-sensitive cone pairs					
33	24	26*	7·4	169	663	98	170	30	31
34	54	26	0·4	41	163	25	43	8	8
Mean	39	26	3·9	105	413	62	107	19	20

The Table summarizes the estimates of basic constants determined from observations of cell separation, mean space constant ($\bar{\lambda}$) and mutual resistance (R_μ). r_m is the resistance between the inside and outside of an isolated cone and R_m is this resistance × unit area calculated for the continuous sheet model. R_s is the sheet resistance and r_s the coupling resistance between cones. For the square array $r_s = R_s$; the values of r_s shown above are for the hexagonal array where $r_s = 3^{\frac{1}{2}}R_s$. The last columns give the input resistance (r_{in}) calculated for the square and hexagonal arrays. The results are listed in order of decreasing membrane resistance, first red–red pairs and then green–green pairs. Some experiments were performed in the early stages of the investigation when a defective prism blurred the image of the slit and made λ measurements unreliable. In these instances, indicated by an asterisk, we have used the mean value of λ determined on a large number of cones with the faulty prism replaced.

Since some pairs of red-sensitive cones were uncoupled, it could be argued that the absence of coupling amongst the red–green pairs is a fortuitous result. However, the probability of this happening by chance is exceedingly low. If we consider the cones separated by less than 60 μm, only four out of thirty-eight pairs of red–red or green–green pairs were uncoupled, so that we may take the chance of finding an uncoupled

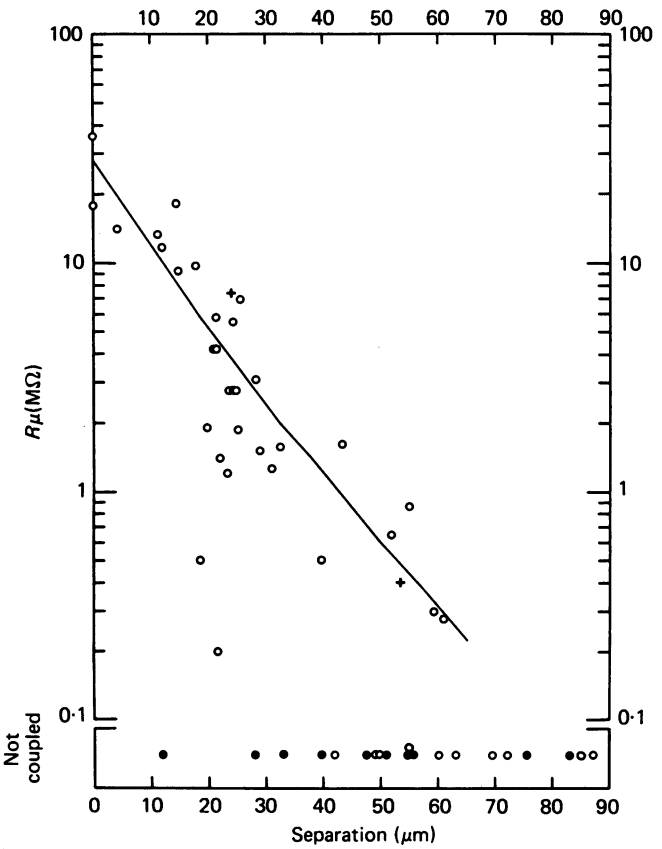

Text-fig. 5. Mutual resistance R_μ *vs.* cell separation in fifty-four pairs of cones, ○, red–red cone pairs; +, green–green cone pairs; ●, red–green cone pairs. The line is drawn from the theory for a hexagonal array with $\lambda = D = 17{\cdot}4$ μm and $r_m = 100$ MΩ using eqns. (8) and (6). Note: $R_\mu = V_r/i_o$.

pair of similar cones separated by less than 60 μm as about 1/9·5. If dissimilar cones, i.e. red–green pairs, were just as likely to be coupled as pairs of similar spectral sensitivity, the chance of finding all eight uncoupled at a separation less than 60 μm is only 1 in $9{\cdot}5^8$. The argument is not as strong as this, because the psychological incentive to complete the measurement of cone separation was greater when the cones were coupled than when they were not. However, even when allowance is made for some bias toward selecting coupled cones, the sample does provide good evidence that coupling is only between cones of the same spectral sensitivity. This statement applies to red- and green-sensitive cones. No blue-sensitive cone was encountered in the present work, and as far as we know there is no evidence, either

direct or indirect, as to whether blue-sensitive cones are coupled to one another. Their spectral sensitivity (Tomita, Kaneko, Murakami & Pautler, 1967; Baylor & Hodgkin, 1973) makes it unlikely that they are coupled to red- or green-sensitive cones.

TABLE 4. Cone pairs with no detectable coupling

Red–red cone pairs*

Separation (μm)	Red cone I $\bar{\lambda}$ (μm)	Red cone II $\bar{\lambda}$ (μm)
42	21	23
49	25	28
49	22	15
55	27	24
60	—	—
63	—	—
70	—	—
72	28	24
85	32	29
87	—	—

Red–green cone pairs*

Separation (μm)	Red cone $\bar{\lambda}$ (μm)	Green cone $\bar{\lambda}$ (μm)
12	—	—
28	26	27
33	—	—
40	28	39
48	37	32
51	28	21
54	16	23
56	—	—
76	—	—
83	29	27

* Cells without space constants were recorded with a low quality prism in the optical stimulator which made the measurements unreliable (see Table 2).

As can be seen from Text-fig. 5, in two instances the abscissa is zero, which means that both electrodes were considered to be in the same cell. The evidence for this comes from the coincidence of spatial profiles in both cases and in one case from the additional evidence of dye marking. In these two experiments as well as in others in which the electrodes were very close to one another we noticed that the resting potential and light response fell abruptly by several millivolts when the second microelectrode was inserted. The inference is that insertion of two microelectrodes, and in all probability insertion of one, causes a leak, which reduces the resting potential and light response. It is therefore likely that the mutual resistances given in Table 2 are lower than they would be in undisturbed cones.

Text-fig. 5 shows two instances where red cones were separated by about 20 μm but had very low mutual resistances. In both cases the cells involved had normal spatial profiles, responded well to light, and did not appear to be damaged. Weak coupling over such a short distance could be due to a failure in the direct continuity

of the network. The presence of electrically isolated (uncoupled) cells (Baylor & Hodgkin, 1973; Lamb & Simon, 1977) indicates that the network is not complete. Hence it is possible that in some instances the electrical interaction between neighbouring cells takes place over a circuitous path with a high resistance rather than a direct path with a low resistance.

We never saw a case in which the mutual resistance was negative, i.e. in which current caused a voltage of opposite polarity in the other member of the cone pair. However, as Baylor *et al.* (1971) observed reverse coupling in only one out of twelve pairs of coupled cones, our failure to see reverse coupling in thirty-four coupled pairs is not incompatible with their results.

Some miscellaneous observations

There were two instances in which cells that had been impaled with two electrodes gave slow depolarizations of a few millivolts with long latencies in response to large-diameter bright flashes. It seems likely that on both occasions the late depolarization was a synaptic potential coming from activation of the horizontal cell feed-back loop. The disappearance of the normal hyperpolarizing light response upon insertion of the second electrode suggests that electrical connexions of the inner segment to its outer segment and to the rest of the receptor network were broken in the process. That the chemical junctions between the cone and horizontal cell were not disrupted may indicate that they are located on a different part of the receptor or that they are more robust than the electrical junctions.

On one occasion the penetration of what was originally identified as a red-sensitive cone by a second electrode caused the cell to become sensitive to red and green lights. Cells that have both red and green spectral sensitivities have been identified as double cones (Richter & Simon, 1974; Baylor & Fettiplace, 1975). It is conceivable then that the cell we initially thought to be a red cone was in fact the red member of a double cone which was electrically isolated from its green member. Insertion of the second electrode may have created a junction between the red- and green-sensitive regions. Such an explanation raises the possibility that the red and green members of undamaged double cones behave as independent elements, i.e. as a red cone or green cone depending on the electrode placement. This could be the reason that double cones, which are identified on the basis of spectral sensitivity, appear to be recorded so rarely despite their large size and fair abundance (Baylor & Fettiplace, 1975).

Calculation of electrical constants

How appropriate is the model used for calculation? In a retina like that of *Bufo marinus* where there are few cones, the rods are arranged in a fairly regular hexagonal array (personal communication from Dr G. Gold and our own observations). By 'fairly regular' we mean that in the great majority of instances each rod is surrounded by six nearest neighbours. Since connections between rods are thought to be through gap junctions on the buttresses of adjacent inner segments (Fain, Gold & Dowling, 1975), there is good reason to think that in an all-rod retina the hexagonal model used by Lamb & Simon (1976) and ourselves may provide a good basis for calculating electrical constants. We are on less sure ground when applying the model to an array of red- or green-sensitive cones. Even if the cones themselves are arranged hexagonally the colour sensitivity, which is shown by the oil droplets in reptiles, seems to be distributed in a random way, judged by Text-fig. 6, which is based on a photograph taken by Baylor & Fuortes (see Hodgkin, 1971, Text-fig. 2). Moreover, connections between cones are probably made by basal processes (see p. 98) which may cross one another and link many cones in an irregular way.

An attempt was made to characterize the array of red-sensitive cones in Text-fig. 6

by the following procedure. It was assumed, arbitrarily, that the connections between cones do not cross, and with this reservation, that all possible connections are made. This procedure necessarily generates a pattern like that in Text-fig. 6, in which the space is divided into a series of irregular triangles. We attempted to follow a regular procedure, starting by joining those cones that are closest to one another, then proceeding to the next closest pair and so on. In practice the procedure is somewhat arbitrary, particularly as it is difficult to decide which cones should be regarded as on the edge. In the field of 103 red cones shown in Text-fig. 6 the average number of connexions per red cone for one pattern was found to be 5·9 with a standard deviation of 1·4; the number of connexions per cone ranged between 4 and 10.

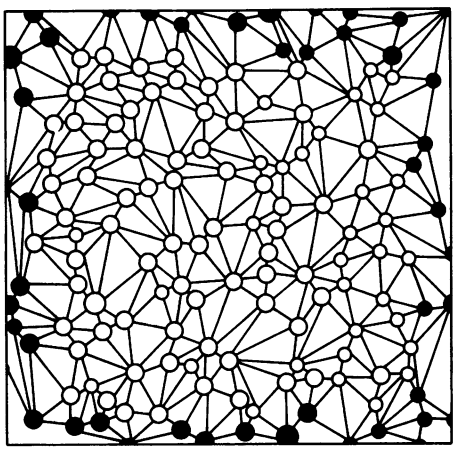

Text-fig. 6. A pattern of possible connexions between red cones. The relative positioning of a field of red cones was mapped by tracing a circle around each of the red oil drops in Fig. 2 of Hodgkin (1971). See text for the procedure used to draw the lines connecting cones. Not counting the cells on the edge (filled circles), this pattern had a mean of 5·9 connexions per cone.

Estimate of electrical constants made from average data. An estimate of the approximate magnitude of the cell constants can be made from the data in Text-fig. 5, in which mutual resistance is plotted against separation. In this Figure the continuous line was calculated by eqn. (8) for the hexagonal array with $\lambda = D = 17{\cdot}4\ \mu m$ (the effective spacing of red-sensitive cones) and with $r_m = 100\ M\Omega$. As the line is reasonably close to the resistances of most of the more tightly coupled cones, it appears that the cell resistance is of the order of 100 MΩ, and from eqns. (1) and (4), that R_m is about 300 Ωcm^2 and R_s about 100 MΩ. For a hexagonal array, r_s would be 173 MΩ. The input resistance which is given by the intercept of the line with the axis, is 28 MΩ.

Although approximate, the above method has the advantage that it does not rely on estimation of the space constant, λ, from spatial profiles, a procedure that might give errors if these profiles are seriously modified by light scattering.

Calculation of electrical constants in individual experiments. Each successful experiment gave estimates of the following three quantities: (1) the separation of the two cones, (2) their mutual resistance, (3) their mean space constant, λ. From these three

quantities and the effective distance, D, between cones of the same spectral sensitivity, we can calculate the membrane resistance, r_m, of an isolated cone, the coupling resistance, r_s, between them, and the input resistance, r_{in}. The method of calculation and the equations used are summarized in the example on p. 80. With the approximations used the value calculated for r_m is the same for hexagonal and square models, but for r_s is $\sqrt{3}$ times greater when the hexagonal model is used for calculation. The calculated value of the sheet resistivity, R_s, is the same for both models and may be a better quantity to tabulate.

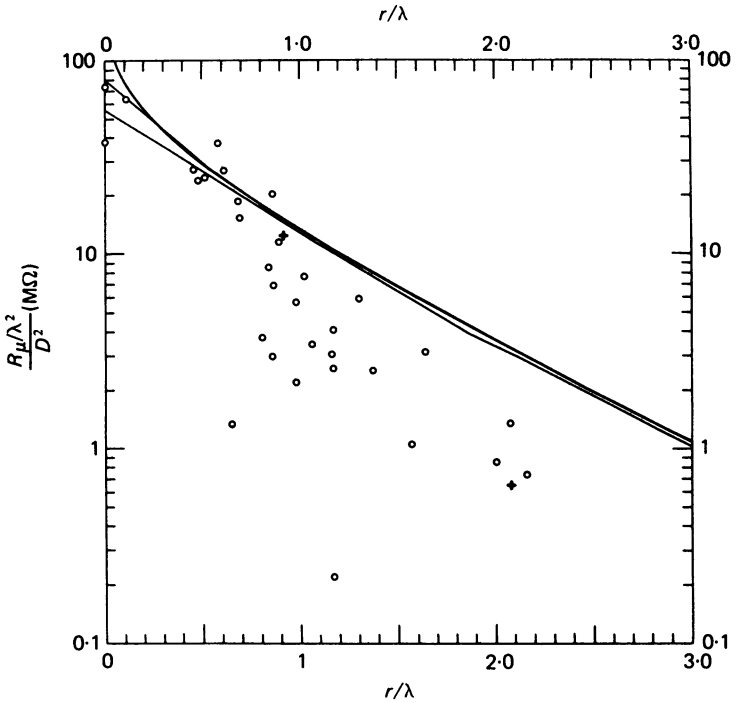

Text-fig. 7. Data of Fig. 5 'normalized' by plotting $R_\mu \frac{\lambda^2}{D^2}$ against $\frac{r}{\lambda}$ (see Fig. 2). The lines, from top downwards, are for $\frac{\lambda}{D} = \infty$ (continuous sheet model): $\frac{\lambda}{D} = 2$, hexagonal array, and $\frac{\lambda}{D} = 1$, hexagonal array. $r_m = 200$ MΩ throughout. All points should fall close to the theoretical curves if r_m and D were the same in all preparations but r_s varied from cone to cone. Note $R_\mu = V_r/i_o$.

Table 3 summarizes the results. The highest values of r_m, which are perhaps the most reliable (as electrode damage may lower resistance), are in the range 100–300 MΩ; this is roughly consistent with the value of 170 MΩ obtained by Baylor, Hodgkin & Lamb (1974, Table 2) which they considered might have been obtained on an isolated cone.

As has been mentioned previously the low membrane resistances calculated for pairs 31 and 32 might be attributed to breaks or irregularities in the network, or to the existence of overlapping networks. With the exception of these pairs the range of variation is no greater than that often found in the measurements of the membrane

resistance of single nerve fibres (Cole & Hodgkin, 1939; Hodgkin & Rushton, 1946; Hodgkin, 1947; Weidmann, 1951). An additional source of error must be introduced by the probable variation in the number of connexions per cone illustrated in Text-fig. 6.

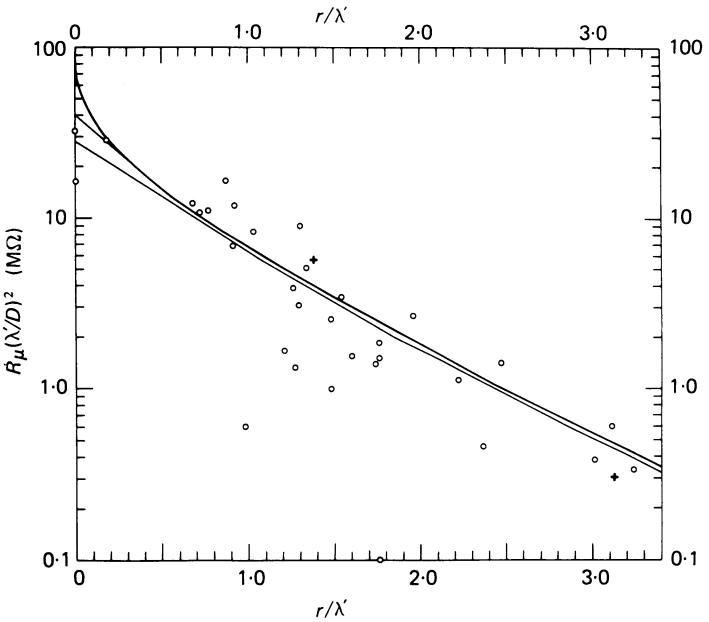

Text-fig. 8. Same plot as in Fig. 7 but using a new space constant (λ'), assumed to be 2/3 of the measured space constant λ. r_m was taken as 100 MΩ in drawing the theoretical curves, which are as in Fig. 7 from top to bottom $\frac{\lambda'}{D} = \infty$, $\frac{\lambda'}{D} = 2$ and $\frac{\lambda'}{D} = 1$.

Discrepancies in the analytical approach

The mean space constant determined in the illuminated strip experiments on eighty-three red-sensitive cones was 25 μm. In Text-fig. 5 on the other hand, a moderately good fit to the more tightly coupled cones was drawn with $\lambda = D =$ 17·4 μm. A line drawn from the theoretical equations for a hexagonal or square array with $\lambda = 1{\cdot}5\ D = 26\ \mu$m was found to be a poor fit to the same data.

Text-fig. 7 illustrates a different way to bring out the discrepancy. Here the quantity $R_\mu(\lambda^2/D^2)$ has been plotted against r/λ so that the data can be compared with the curve for the continuous-sheet model shown in Text-fig. 2 or with the lines for $\lambda/D = 1$ and 2 for the hexagonal array. If it is assumed that all cells have the same total membrane resistance, r_m, but that different pairs differ in the amount of coupling, then this method of plotting should bring all the points close to the theoretical curves. This prediction was not fulfilled, as the points in Text-fig. 7 fall off more quickly than the theoretical curves.

Another less plausible approach is to assume that the sheet resistivity is constant and that variations in λ are caused by variations in the membrane resistance, R_m. In that case a plot of R_μ against r/λ should bring all the points close to the theoretical curve. This was tried but the fit was no better than in Text-fig. 7.

One way of explaining the discrepancy is to assume that the curve for light scattering from a line source contains two components. The first component, which will be considered on p. 94, has a Gaussian shape and a scattering coefficient, σ, of about 10 μm as found by Schwartz (1973). It will be shown later (p. 94) that

TABLE 5. Influence of error in λ on basic constants

	Pair	Separation (μm)	λ (μm)	R_μ (MΩ)	r_m (MΩ)	r_s (MΩ)	r_{in} (MΩ)
			Red-sensitive pairs				
	1	15	25	18	290	243	48
	1*	15	17*	18	240*	454*	71*
	2	26	30	6·9	247	147	32
	2*	26	20*	6·9	263*	352*	60*
	4	0	25	36	215	183	36
	4*	0	17*	36	153*	249*	45*
Mean	1–16	20	29	10	167	114	24
	1*–16*	20	19*	10	149*	221*	38*
Mean	1–32	26	27	6	109	79	16
	1*–32*	26	18*	6	107*	172*	28*
			Green-sensitive pairs				
	33	24	26	7·4	169	170	31
	33*	24	17*	7·4	164*	371*	56*
	34	54	26	0·4	41	43	8
	34*	54	17*	0·4	73*	168*	25*

The Table shows the effect of assuming that light scattering has increased λ by 50 % on calculated values of r_m and other constants. In the upper line of each pair the value is based on Table 1 and is calculated from the uncorrected λ; in the lower line (e.g. 1*) it is assumed that λ' was 2/3 of the observed λ. The revised constants that result from this assumption are marked with an asterisk. The values of r_s and r_{in} are for the hexagonal array. The selection of cones 1–16 is an arbitrary attempt to exclude damaged cells or lightly coupled cells to which the theory would be less applicable.

scattering of this kind should not alter the value of λ determined from the asymptotes on a semilogarithmic curve. However, if the scattering function had a broad skirt, in addition to its relatively sharp centre (see Copenhagen & Owen, 1976), then the values of λ might be erroneously high. Text-fig. 8 shows that this could explain the discrepancy. Here λ' has been taken as 2/3 of λ, and with this modification the values of $(\lambda'/D)^2 R_\mu$ do not deviate systematically from the theoretical curve when plotted against r/λ'. Table 5 shows the effect of reducing λ by 1/3 on the calculated value of r_m and other constants.

Effect of simple light scattering on the form of the spatial profile

By simple light scattering we mean that for each illuminated point the distribution due to light scatter is Gaussian, as assumed by Baylor *et al.* (1971) and Schwartz (1973), and that the distribution has a standard deviation of about 10 μm. In practice light scattering is probably more complicated and the distribution about an illuminated point may include a wider skirt, such as that shown in Text-fig. 12 of

Copenhagen & Owen (1976). Unfortunately no one has yet devised a satisfactory direct method of measuring light scattering in the retina. In this section we are concerned only with the simple Gaussian light scattering and will attempt to answer two related questions. First, are the rounded tops of spatial profiles such as those in Text-figs. 4 and 9 consistent with Gaussian scatter, and if so what is the scatter coefficient? Secondly, is this amount of scattering likely to affect the method of measuring the space constant, λ?

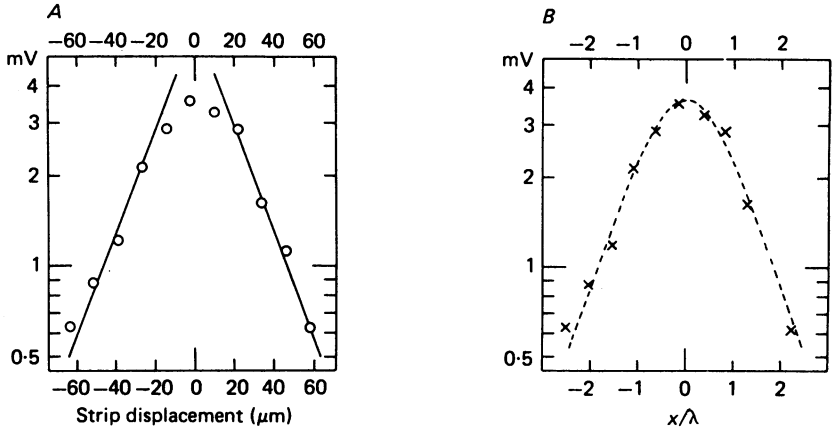

Text-fig. 9. Comparison of a spatial-sensitivity profile and a theoretical expression that allows for light scattering. *A*, peak amplitude plotted on a logarithmic scale against strip displacement. Straight lines were fitted to the points by eye and had slopes that corresponded to $\lambda = 24{\cdot}8$ μm for both positive and negative displacements. The stimulus was a flash of 650 nm light that delivered $1{\cdot}5 \times 10^3$ photons μm^{-2} to a strip 1·55 mm by 5 μm wide. *B*, same data as *A* except the abscissa is x/λ. The dashed curve allows for scatter and is eqn. 22 with $L = 0{\cdot}8$. This gives a scattering coefficient of $\sigma = 14$ μm. $V_{max} = 17$ mV; temperature 23 °C.

It will be assumed that the distribution of scattered light at the receptor layer from a point source of strength, Q, is

$$F(r) = \frac{Q}{\pi l^2} e^{-r^2/l^2} \tag{16}$$

where r is the distance from the illuminated point, Q is the total quantity of light applied per unit time, i.e. quanta sec^{-1}, and l is a length constant related to the scatter coefficient, σ, by

$$l = 2^{\frac{1}{2}}\sigma. \tag{17}$$

It follows from this that a unit line source of strength, Q', per unit length located at $x = 0$ will give a distribution

$$F(x) = \frac{Q'}{\pi^{\frac{1}{2}} l} e^{-x^2/l^2}, \tag{18}$$

where Q' is in quanta sec^{-1} μm^{-1}.

If there were no light scatter a line source applied to an array of cones would, on the continuous-sheet model, produce a voltage, V, given by the following equation:

$$V(x) = \frac{Q'S}{2\lambda} e^{-|x/\lambda|}, \tag{19}$$

where S is the steady-state sensitivity when a large area is illuminated.

In the presence of light scattering defined by (18), the distribution in (19) will be changed to

$$V(x, l) = Q'S\left\{\frac{1}{2\lambda} e^{-|x/\lambda|}\right\} * \left\{\frac{1}{l\pi^{\frac{1}{2}}} e^{-x^2/l^2}\right\}, \tag{20}$$

where $*$ implies the convolution of one function with another, i.e.

$$V(x, l) = \int_{-\infty}^{\infty} V(x') F(x-x')\, dx'. \tag{21}$$

The integral in (20) can be shown by standard methods to be

$$V(x, L) = \frac{Q'S}{4\lambda} e^{L^2/4}\left\{e^X \operatorname{erfc}\left(\frac{L}{2}+\frac{X}{L}\right) + e^{-X} \operatorname{erfc}\left(\frac{L}{2}-\frac{X}{L}\right)\right\}, \tag{22}$$

where $X = x/\lambda$ and $L = l/\lambda$.

This function was fitted to the experimental curves by a plot of log { } from eqn. (22) against X for different values of L; the family of curves was then compared with the experimental plot of log V against x/λ and the best fit selected by eye (Text-fig. 9). The mean value of l/λ was 0·5 with a standard deviation of 0·22; the mean scatter coefficient, σ, was 9 μm with a standard deviation of 4 μm. The analysis showed that if scattering follows a simple Gaussian curve and if l/λ is about 0·5 there should be little error in the method of measuring λ since eqn. (22) approximates closely to an exponential when $x/\lambda > 1$. However, this does not eliminate the possibility that the values of λ might have been increased by a broad skirt on the light-scattering curve.

Our values of the scatter coefficient, σ, are in reasonable agreement with those of Schwartz (1973) and Copenhagen & Owen (1976), who obtained 10 and 6 μm, respectively.

On several occasions, eqn. (22) could not be fitted at all. There were two kinds of deviation. In some instances the spatial profile was very asymmetrical, with a normal value of λ on one side and a small one on the other; this could be explained if the impaled cone was near the end of a cluster of coupled cones, rather than in the middle of a continuous array. In other instances, particularly with green-sensitive cones, the distribution had a secondary hump or even a double peak, as one might expect if the contribution from neighbouring cones exceeded that of the impaled cone.

Velocity of electrical spread through the cone network. As can be seen from Text-figs. 10 and 11 the crest of the electrical response produced by a flash of light occurs later as the illuminated strip is moved away from the impaled cone. (The velocities measured in fifteen experiments had a mean of 2·7 mm/sec, and a range of 4·3 to 1·7 mm/sec). A possible explanation that may well apply to the largest responses, i.e. to those between ± 25 μm, is that some of the spread is caused by light

scattering and that the record at zero distance had the earliest peak because the light intensity was strongest there and the time to peak decreased with flash intensity.

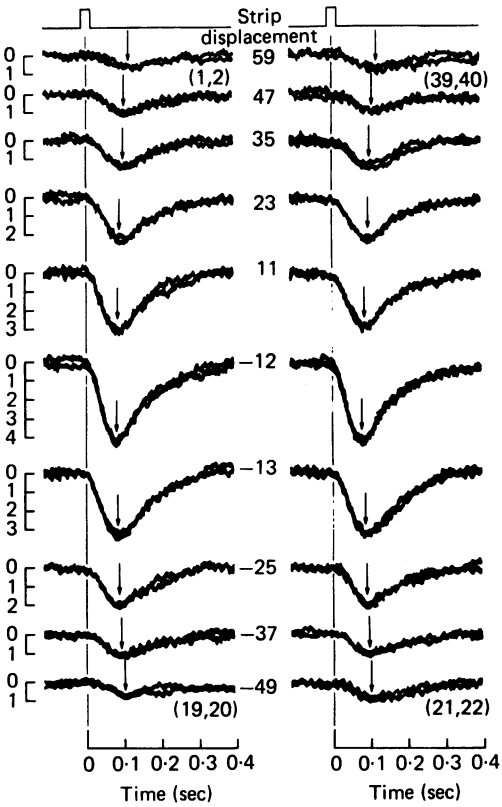

Text-fig. 10. Response as a function of strip displacement. Each frame shows a pair of responses to a 23 msec flash of a strip of 650 nm light ($2{\cdot}9 \times 10^3$ photons μm^{-2}). Stimuli were presented at 2 sec intervals starting at the top of the left column and ending at the top of the right column. The numbers in brackets give the flash number in the sequence. The positive and negative displacement of the strip from the cell centre is given in μm by the numbers in the middle of the Figure. The arrows show the peak amplitude for each response pair. V_{max} 12 mV; temperature 21·7 °C.

However, this is unlikely to be the complete explanation because the effect was seen beyond 25 μm, where the response was small and there should have been little effect from scattered light. In this region the velocity did not seem to vary greatly with the size of the response. Another, more interesting explanation is that the effect depends on the time constant of the cones and that the velocity is determined by the electrical constants λ and τ.

For a wave that is slow compared with the time constant, τ, it can be shown for the continuous-sheet model that the peak of the wave should have a velocity equal to $2\lambda/\tau$, where λ, the space constant, is $(R_m/R_s)^{\frac{1}{2}}$ and τ, the time constant, is $R_m C_m$, where C_m is the capacity per unit area of the sheet; τ is also equal to $r_m c_m$, where c_m is the total capacity between the inside and outside of an isolated cone.

In the continuous-sheet model, the differential equation for one-dimensional electrical spread on either side of a long, narrow strip located at $x = 0$ is

$$\lambda^2 \frac{\partial^2 V}{\partial x^2} = \tau \frac{\partial V}{\partial t} + V. \tag{23}$$

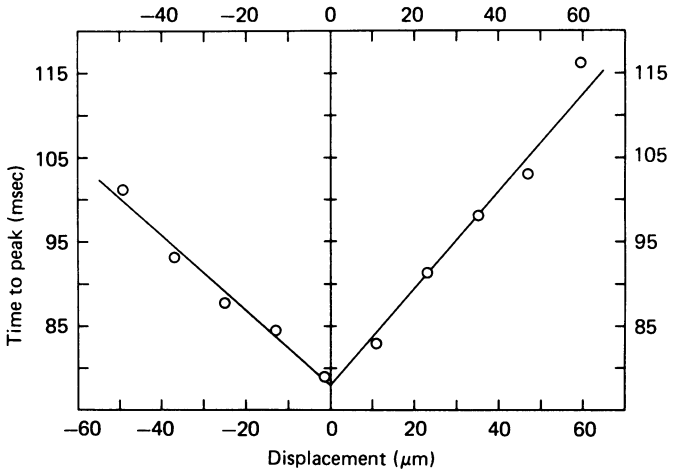

Text-fig. 11. Strip displacement versus time to peak. Same data as in Fig. 10. Straight lines were fitted to the points by eye and had slopes of 1·72 mm/sec for positive displacements and 2·25 mm/sec for negative displacements.

For a sinusoidal input the boundary condition at $x = 0$ may be taken as $V = V_0 e^{j\omega t}$, and the solution is then

$$V = V_0 \exp[j\omega t - (\alpha + \beta j)x] \quad \ldots x > 0, \tag{24}$$

where

$$\alpha = \frac{1}{\lambda\sqrt{2}} [1 + (1 + \tau^2\omega^2)^{\frac{1}{2}}]^{\frac{1}{2}}, \tag{25}$$

$$\beta = \frac{1}{\lambda\sqrt{2}} [-1 + (1 + \tau^2\omega^2)^{\frac{1}{2}}]^{\frac{1}{2}}. \tag{26}$$

As $\omega \to 0$, i.e. $\omega \ll 1$,

$$\alpha \doteqdot \frac{1}{\lambda} \tag{27}$$

$$\beta \doteqdot \frac{\tau\omega}{2\lambda}. \tag{28}$$

Hence at very low frequencies eqn. (24) becomes

$$V = V_0 \exp(-x/\lambda) \exp\left[jw\left(t - \frac{\tau x}{2\lambda}\right)\right], \tag{29}$$

which implies that the peak attenuates as $e^{-x/\lambda}$ and travels with a velocity of $2\lambda/\tau$. Using the mean velocity of 2·7 mm/sec and the mean λ of 26·5 μm, we obtained a τ of 19·6 msec.

Our value of τ is substantially greater than the time constant of 4–7 msec obtained by Baylor *et al.* (1974), who used a bridge circuit to pass current through, and record from, a single electrode in red-sensitive cones. However, in a coupled network, if voltage is recorded from the cell where current is injected the time for the potential to reach half its final value is much shorter than in an isolated cell. From Table 1, it can be seen that with $\lambda/D = 1{\cdot}5$ the time t_e for $V_{0,0}$ to reach 0·63 of its final value is about $\tau/5$ instead of τ as in an isolated cell. Our observation showed that cone pairs separated by less than 15 μm had values of t_e between 3 and 9 msec whereas those separated by 20–55 μm had values of t_e between 17 and 20 msec. The average time constant obtained by analysing these data with theoretical tables similar to that in Table 1 was 21 msec. This agrees fairly well with the value of 13–18 msec obtained by Hodgkin & O'Bryan (1977) and with the present value of 19·6 msec based on the velocity of electrical spread. The value calculated for the total membrane capacity is about 100 pF which corresponds to about 1·7 μF/cm^2 if the total area is taken as 6×10^{-5} cm^2 (Baylor *et al.* 1974).

DISCUSSION

The results in this paper show that, in the peripheral parts of the turtle's retina, cones are electrically coupled to cones of the same spectral sensitivity but not to others of different spectral sensitivity. Blue-sensitive cones are impaled so rarely that we have no evidence about them but it seems that the two other main types are connected in separate networks of red- and green-sensitive cones. Since neighbouring cells of the same spectral type can be separated by relatively large distances (Text-fig. 6) it seems unlikely that a two dimensional network could be formed solely by gap junctions between cell bodies. This suggests that electrical junctions are made between the basal processes which radiate over a distance of 10–40 μm in a horizontal plane from the synaptic pedicles (Lasansky, 1971). Evidence which supports this contention is provided by the discovery of gap junctions between the basal processes of cones in the peripheral retina of mammals (Raviola & Gilula, 1973).

The demonstration that coupling is between cones of the same spectral identity is consistent with Baylor & Hodgkin's finding (1973) that green-sensitive cones are insensitive to illumination with wavelengths which are optimal for red-sensitive cones. The result seems logical since one would not expect information about colour to be discarded by mixing up cones of different spectral identity in a single network. It is then rather surprising that several morphological studies have demonstrated apparent connexions between cones of different spectral sensitivity as well as between rods and cones (Missotten, Apelmanns & Michiels, 1963; Nilsson, 1964; Cohen, 1965; Sjöstrand, 1969; Raviola & Gilula, 1973; Scholes, 1975). The functional significance of these connexions remains to be worked out. Cells connected by gap junctions can be uncoupled by a variety of experimental procedures, which have only slight or subtle effects on the morphology of the junction (Peracchia & Dulhunty, 1976; Peracchia, 1977). It therefore seems probable that not all junctions identified histologically as gap junctions are operative as electrical links and that electron-microscopy needs to be supplemented with electrical measurements before one can decide whether cells are connected together or not.

A complete experiment on a pair of coupled cones gave their separation, mutual resistance and space constant; in some cases we also obtained information about the time constant of the network. From this information and an appropriate model one can calculate basic quantities such as the resistance or capacity between the inside and outside of an isolated cone and the value of the resistance linking cones together. Since the theory is more likely to apply when cones are tightly coupled, and as injury probably reduces the membrane resistance, we consider that the first sixteen cones out of the total of thirty-two red-sensitive cones in Table 3 may give a better value than the overall average. These gave an average mutual resistance of 29 MΩ at a mean separation of 20 μm and a mean space constant of 29 μm. The average value of the membrane resistance r_m was 167 MΩ; the mean coupling resistance r_s was 66 MΩ for the square array and 114 MΩ for a hexagonal array; the input resistance of a cone in the network was 24 MΩ. A smaller number of experiments gave the membrane time constant as 20 msec and the total capacity of an isolated cone as about 100 pF. These values are in fair agreement with estimates made by Lamb & Simon (1976), Baylor *et al.* (1974) and Hodgkin & O'Bryan (1977).

We are greatly indebted to Dr T. D. Lamb for much helpful discussion and for writing the computer programmes on which Text-figs. 1 and 2 and Table 1 are based. Our thanks are also due to Mr W. W. Stewart for providing Lucifer yellow and to Mr R. H. Cook for building the optical stimulator. This investigation was supported by grant 1R01 EY02078-01 from the National Eye Institute, U.S.P.H.S.

REFERENCES

BAYLOR, D. A. & FETTIPLACE, R. (1975). Light path and photon capture in turtle photoreceptors. *J. Physiol.* **248**, 433–464.

BAYLOR, D. A., FUORTES, M. G. F. & O'BRYAN, P. M. (1971). Receptive fields of cones in the retina of the turtle. *J. Physiol.* **214**, 265–294.

BAYLOR, D. A. & HODGKIN, A. L. (1973). Detection and resolution of visual stimuli by turtle photoreceptors. *J. Physiol.* **234**, 163–198.

BAYLOR, D. A., HODGKIN, A. L. & LAMB, T. D. (1974). The electrical response of turtle cones to flashes and steps of light. *J. Physiol.* **242**, 685–727.

CARSLAW, H. S. & JAEGER, J. C. (1959). *Conduction of Heat in Solids*, 2nd edn. Oxford: University Press.

COHEN, A. I. (1965). Some electron microscopic observations on interreceptor contacts in the human and macaque retina. *J. Anat.* **99**, 595–610.

COLBURN, T. R. & SCHWARTZ, E. A. (1972). Linear voltage control of current passed through a micropipette with variable resistance. *Med. Electron. & biol. Engng* **10**, 504–509.

COLE, K. S. & HODGKIN, A. L. (1939). Membrane and protoplasm resistance in the squid giant axon. *J. gen. Physiol.* **22**, 671–687.

COPENHAGEN, D. R. & OWEN, W. G. (1976). Functional characteristics of lateral interactions between rods in the retina of the snapping turtle. *J. Physiol.* **259**, 251–282.

FAIN, G. L., GOLD, G. H. & DOWLING, J. E. (1975). Receptor coupling in the toad retina. *Cold Spring Harbor Symp. quant. Biol.* **40**, 547–561.

HODGKIN, A. L. (1947). The membrane resistance of a non-medullated nerve fibre. *J. Physiol.* **106**, 305–318.

HODGKIN, A. L. (1971). Address of the President, Professor A. L. Hodgkin, at the Anniversary Meeting, 30 November 1971. *Proc. R. Soc.* A **326**, v–xx.

HODGKIN, A. L. & O'BRYAN, P. M. (1977). Internal recording of the early receptor potential in turtle cones. *J. Physiol.* **267**, 737–766.

HODGKIN, A. L. & RUSHTON, W. A. H. (1946). The electrical constants of a crustacean nerve fibre. *Proc. R. Soc.* B **133**, 444–479.

JACK, J. J. B., NOBLE, D. & TSIEN, R. W. (1975). *Electric Current Flow in Excitable Cells*, p. 88. Oxford: Clarendon.

LAMB, T. D. (1976). Spatial properties of horizontal cell responses in the turtle retina. *J. Physiol.* **263**, 239–255.

LAMB, T. D. & SIMON, E. J. (1976). The relation between intercellular coupling and electrical noise in turtle photoreceptors. *J. Physiol.* **263**, 257–286.

LAMB, T. D. & SIMON, E. J. (1977). Analysis of electrical noise in turtle cones. *J. Physiol.* **272**, 435–468.

LASANSKY, A. (1971). Synaptic organization of cone cells in the turtle retina. *Phil. Trans. R. Soc.* B **262**, 365–381.

MISSOTTEN, L., APELMANNS, M. & MICHIELS, J. (1963). L'ultrastructure des synapses des cellules visuelles de la rétine humaine. *Bull. Mém. Soc. franc. ophthal.* **76**, 59–82.

NILSSON, S.-E. G. (1964). Interreceptor contacts in the retina of the frog (*Rana pipiens*). *J. Ultrastruct. Res.* **11**, 147–165.

PERACCHIA, C. (1977). Gap junctions structural changes after uncoupling procedures. *J. cell Biol.* **72**, 628–641.

PERACCHIA, C. & DULHUNTY, A. (1976). Low resistance junctions in crayfish structural changes with functional uncoupling. *J. cell Biol.* **70**, 419–439.

RAVIOLA, E. & GILULA, B. N. (1973). Gap junctions between photoreceptor cells in the vertebrate retina. *Proc. natn. Acad. Sci. U.S.A.* **70**, 1677–1681.

RICHTER, A. & SIMON, E. J. (1974). Electrical responses of double cones in the turtle retina. *J. Physiol.* **242**, 673–684.

SCHOLES, J. H. (1975). Colour receptors, and their synaptic connexions, in the retina of a cyprinid fish. *Phil. Trans. R. Soc.* B **270**, 61–118.

SCHWARTZ, E. A. (1973). Responses of single rods in the retina of the turtle. *J. Physiol.* **232**, 503–514.

SJÖSTRAND, F. S. (1969). The outer plexiform layer and the neural organization of the retina. In *The Retina: Morphology, Function and Clinical Characteristics*, U.C.L.A. Forum in Medical Sciences 8, ed. STRAATSMA, B. R., HALL, M. O., ALLEN, R. A. & CRESCITELLI, F., pp. 63–100. Berkeley and Los Angeles: University of California Press.

STEWART, W. W. (1978). Functional connections between cells as revealed by dye-coupling with a highly fluorescent naphthalimide tracer. *Cell* **14**, 741–759.

TOMITA, T., KANEKO, A., MURAKAMI, M. & PAUTLER, E. L. (1967). Spectral response curves of single cones in the carp. *Vision Res.* **7**, 519–531.

WEIDMANN, S. (1951). Electrical characteristics of *Sepia* axons. *J. Physiol.* **114**, 372–381.

EXPLANATION OF PLATE

A, photomicrograph of a pair of fluorescently stained cells in the intact retina. Two cones were impaled with electrodes containing the fluorescent compound Lucifer yellow. The separation between cells, estimated from the spatial sensitivity profiles, was 54 μm. Both cells were then injected with Lucifer and after fixation with formaldehyde the piece of eyecup containing them was viewed with a compound microscope from the vitreal surface using incident illumination. Along this optical axis the marked cells appear as fluorescent circles having a centre-to-centre separation of 55 μm. *B*, the same cells as in *A* after being embedded and sectioned. The drawings confirm that the cells in *A* are cones. The calibration bar represents 20 μm in *A* and 5·5 μm in *B*.

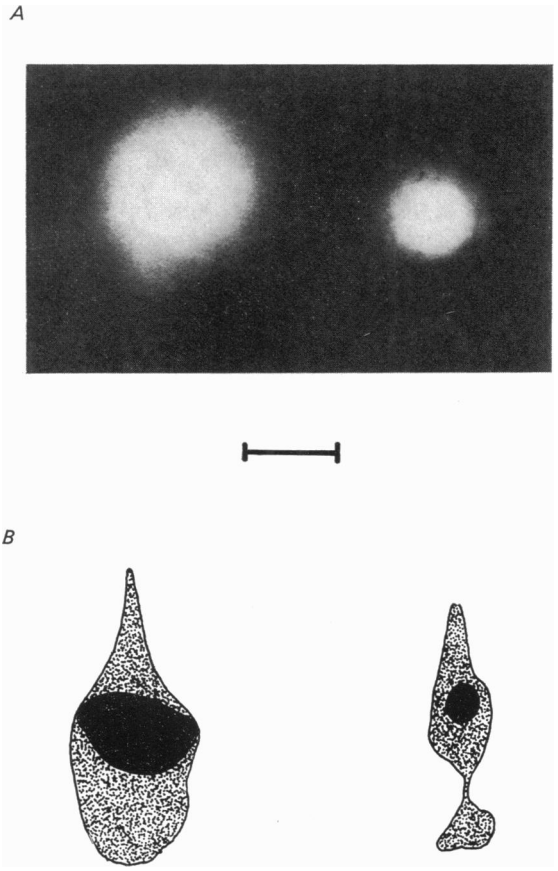
A
B